

Two-species fermion mixtures with population imbalance

M. Iskin and C. A. R. Sá de Melo

School of Physics, Georgia Institute of Technology, Atlanta, Georgia 30332, USA

(Dated: February 8, 2020)

We analyze the phase diagram of uniform superfluidity for two-species fermion mixtures from the Bardeen-Cooper-Schrieffer (BCS) to Bose-Einstein condensation (BEC) limit as a function of the scattering parameter and population imbalance. We find at zero temperature that the phase diagram of population imbalance versus scattering parameter is asymmetric for non-equal masses, having a larger stability region for uniform superfluidity when the lighter fermions are in excess. In addition, we find topological quantum phase transitions associated with the disappearance or appearance of momentum space regions of zero quasiparticle energies. Lastly, near the critical temperature, we derive the Ginzburg-Landau equation, and show that it describes a dilute mixture of composite bosons and unpaired fermions in the BEC limit.

PACS numbers: 03.75.Ss, 03.75.Hh, 05.30.Fk

Major experimental breakthroughs have been made recently involving one-species trapped fermions (${}^6\text{Li}$) in two hyperfine states with different populations. The superfluid to normal phase transition and the vortex state [1], as well as phase separation between paired and unpaired fermions [2] were identified as a function of population imbalance and scattering parameter. These studies are important extensions of the so-called Bardeen-Cooper-Schrieffer (BCS) to Bose-Einstein condensation (BEC) evolution for equal populations, which were studied via the use of Feshbach resonances [3, 4, 5, 6, 7]. The problem of fermion superfluidity with population imbalance has been revisited recently in several theoretical works in continuum [8, 9, 10, 11, 12, 13, 14] and trapped [15, 16, 17, 18, 19] atoms. These one-species experiments are ideal candidates for the observation of uniform and non-uniform superfluid phases, which may be present not only in atomic, but also in nuclear (pairing in nuclei), astrophysics (neutron stars), and condensed matter (superconductors) systems.

Arguably one of the next frontiers of exploration in ultracold Fermi systems is the search for superfluidity in two-species fermion mixtures (e.g. ${}^6\text{Li}$ and ${}^{40}\text{K}$) with and without population imbalance. While earlier works on two-species fermion mixtures were limited to the BCS limit [20, 21], in this manuscript we study the evolution of superfluidity from the BCS to the BEC limit as a function of the scattering parameter and population imbalance.

Our main results are as follows. At zero temperature ($T \approx 0$), we construct the phase diagram for uniform superfluidity involving equal and non-equal masses of paired fermions as a function of scattering parameter $1/(k_{F,+}a_F)$ and population imbalance P as shown in Fig. 1. The phase diagram is asymmetric for non-equal masses, having a larger stability region for uniform superfluidity when the lighter fermions are in excess. The unstable (stable) regions of uniform superfluidity are characterized by a negative (positive) superfluid density. In addition, we find topological quantum phase transitions

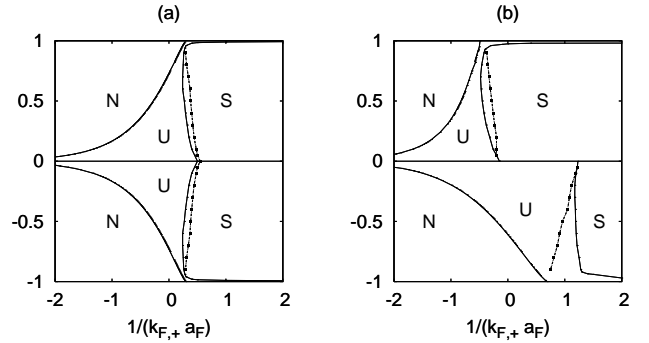


FIG. 1: Phase diagram of population imbalance P versus $1/(k_{F,+}a_F)$ for a) equal ($m_{\uparrow} = m_{\downarrow}$) and b) non-equal masses ($m_{\uparrow} = 0.15m_{\downarrow}$). The symbols N , S and U stands for normal, stable and unstable uniform superfluid phases, respectively. The dotted lines separate topologically distinct regions.

associated with the disappearance or appearance of momentum space regions of zero quasiparticle energies when either $1/(k_{F,+}a_F)$ or P is changed. Lastly, near the critical temperature, we derive the time-dependent Ginzburg-Landau (TDGL) equation, and show that it describes a dilute mixture of bosons (tightly bound fermions) and excess (unpaired) fermions in the BEC limit.

To describe a dilute two-species Fermi gas in three dimensions, we start from the pseudo-spin singlet Hamiltonian ($\hbar = 1$)

$$H = \sum_{\mathbf{k},\sigma} \xi_{\mathbf{k},\sigma} a_{\mathbf{k},\sigma}^{\dagger} a_{\mathbf{k},\sigma} + \sum_{\mathbf{k},\mathbf{k}',\mathbf{q}} V(\mathbf{k},\mathbf{k}') b_{\mathbf{k},\mathbf{q}}^{\dagger} b_{\mathbf{k}',\mathbf{q}}, \quad (1)$$

where the pseudo-spin σ labels the hyperfine states represented by the creation operator $a_{\mathbf{k},\sigma}^{\dagger}$, and $b_{\mathbf{k},\mathbf{q}}^{\dagger} = a_{\mathbf{k}+\mathbf{q}/2,\uparrow}^{\dagger} a_{-\mathbf{k}+\mathbf{q}/2,\downarrow}^{\dagger}$. Here, $\xi_{\mathbf{k},\sigma} = \epsilon_{\mathbf{k},\sigma} - \mu_{\sigma}$, where $\epsilon_{\mathbf{k},\sigma} = k^2/(2m_{\sigma})$ is the energy and μ_{σ} is the chemical potential of the fermions. Notice that we allow for the fermions to have different masses m_{σ} and different populations controlled by independent chemical potentials μ_{σ} . The attractive fermion-fermion interaction $V(\mathbf{k},\mathbf{k}')$ can be writ-

ten in a separable form as $V(\mathbf{k}, \mathbf{k}') = -g\Gamma_{\mathbf{k}}^*\Gamma_{\mathbf{k}'}$ where $g > 0$, and $\Gamma_{\mathbf{k}} = 1$ for the s-wave symmetry considered in this manuscript.

The gaussian effective action for H is $S_{\text{gauss}} = S_0 + (\beta/2)\sum_q \bar{\Lambda}^\dagger(q)\mathbf{F}^{-1}(q)\bar{\Lambda}(q)$, where $q = (\mathbf{q}, v_\ell)$ with bosonic Matsubara frequency $v_\ell = 2\ell\pi/\beta$. Here, $\beta = 1/T$, $\bar{\Lambda}^\dagger(q)$ is the order parameter fluctuation field, and the matrix $\mathbf{F}^{-1}(q)$ is the inverse fluctuation propagator. The saddle point action is

$$S_0 = \beta \frac{|\Delta_0|^2}{g} + \sum_p \left\{ \beta(\xi_{\mathbf{k},+} - E_{\mathbf{k},+}) + \ln[n_F(-E_{\mathbf{k},\uparrow})] + \ln[n_F(-E_{\mathbf{k},\downarrow})] \right\}, \quad (2)$$

where $E_{\mathbf{k},\sigma} = (\xi_{\mathbf{k},+}^2 + |\Delta_{\mathbf{k}}|^2)^{1/2} + s_\sigma \xi_{\mathbf{k},-}$ is the quasi-particle energy ($s_\uparrow = 1$ and $s_\downarrow = -1$) and $E_{\mathbf{k},\pm} = (E_{\mathbf{k},\uparrow} \pm E_{\mathbf{k},\downarrow})/2$. Here, $\Delta_{\mathbf{k}} = \Delta_0\Gamma_{\mathbf{k}}$ is the order parameter, $n_F(E_{\mathbf{k},\sigma})$ is the Fermi distribution and $\xi_{\mathbf{k},\pm} = (\xi_{\mathbf{k},\uparrow} \pm \xi_{\mathbf{k},\downarrow})/2 = k^2/(2m_\pm) - \mu_\pm$, where $m_\pm = 2m_\uparrow m_\downarrow/(m_\downarrow \pm m_\uparrow)$ and $\mu_\pm = (\mu_\uparrow \pm \mu_\downarrow)/2$. Notice that m_+ is twice the reduced mass of the \uparrow and \downarrow fermions, and that the equal mass case corresponds to $|m_-| \rightarrow \infty$. The fluctuation term in the action leads to a correction to the thermodynamic potential, which can be written as $\Omega_{\text{gauss}} = \Omega_0 + \Omega_{\text{fluct}}$ with $\Omega_0 = S_0/\beta$ and $\Omega_{\text{fluct}} = (1/\beta)\sum_q \ln \det[\mathbf{F}^{-1}(q)/\beta]$.

The saddle point condition $\delta S_0/\delta \Delta_0^* = 0$ leads to an equation for the order parameter

$$\frac{1}{g} = \sum_{\mathbf{k}} \frac{|\Gamma_{\mathbf{k}}|^2}{2E_{\mathbf{k},+}} \mathcal{X}_{\mathbf{k},+}, \quad (3)$$

where $\mathcal{X}_{\mathbf{k},\pm} = (\mathcal{X}_{\mathbf{k},\uparrow} \pm \mathcal{X}_{\mathbf{k},\downarrow})/2$ with $\mathcal{X}_{\mathbf{k},\sigma} = \tanh(\beta E_{\mathbf{k},\sigma}/2)$. As usual, we eliminate g in favor of the scattering length a_F via the relation $1/g = -m_+V/(4\pi a_F) + \sum_{\mathbf{k}} |\Gamma_{\mathbf{k}}|^2/(2\epsilon_{\mathbf{k},+})$, where $\epsilon_{\mathbf{k},\pm} = (\epsilon_{\mathbf{k},\uparrow} \pm \epsilon_{\mathbf{k},\downarrow})/2$. The order parameter equation has to be solved self-consistently with number equations $N_\sigma = -\partial\Omega/\partial\mu_\sigma$ which have two contributions $N_\sigma = N_{0,\sigma} + N_{\text{fluct},\sigma}$. $N_{0,\sigma} = -\partial\Omega_0/\partial\mu_\sigma$ is the saddle point number equation given by

$$N_{0,\sigma} = \sum_{\mathbf{k}} \left(\frac{1 - s_\sigma \mathcal{X}_{\mathbf{k},-}}{2} - \frac{\xi_{\mathbf{k},+}}{2E_{\mathbf{k},+}} \mathcal{X}_{\mathbf{k},+} \right) \quad (4)$$

and $N_{\text{fluct},\sigma} = -\partial\Omega_{\text{fluct}}/\partial\mu_\sigma$ is the fluctuation contribution to N given by $N_{\text{fluct},\sigma} = -(1/\beta)\sum_q \{\partial[\det \mathbf{F}^{-1}(q)]/\partial\mu_\sigma\}/\det \mathbf{F}^{-1}(q)$. We define $B_\pm = m_\uparrow\mu_\uparrow \pm m_\downarrow\mu_\downarrow$ to establish general constraints on the magnitude $|\Delta_0|$ of the order parameter for s-wave pairing in the presence of population imbalance ($N_\uparrow \neq N_\downarrow$). Population imbalance is achieved when either $E_{\mathbf{k},\uparrow}$ or $E_{\mathbf{k},\downarrow}$ is negative in some regions of momentum space. Depending on the number of zeros of $E_{\mathbf{k},\uparrow}$ and $E_{\mathbf{k},\downarrow}$ (zero energy surfaces in momentum space), there are four topologically distinct cases: (I)

$E_{\mathbf{k},\sigma}$ has no zeros and $E_{\mathbf{k},-\sigma}$ has two zeros; (II) $E_{\mathbf{k},\sigma}$ has no zeros and $E_{\mathbf{k},-\sigma}$ has only one; (III) both $E_{\mathbf{k},\sigma}$ and $E_{\mathbf{k},-\sigma}$ have only one zero; and (IV) both $E_{\mathbf{k},\sigma}$ and $E_{\mathbf{k},-\sigma}$ have no zeros. The zeros of $E_{\mathbf{k},\sigma}$ occur at real momenta $k_\pm^2 = B_\pm \pm (B_\pm^2 - 4m_\uparrow m_\downarrow |\Delta_0|^2)^{1/2}$ provided that $|\Delta_0|^2 < |B_-|^2/(4m_\uparrow m_\downarrow)$ for $B_+ \geq 0$ and $|\Delta_0|^2 < -\mu_\uparrow\mu_\downarrow$ for $B_+ < 0$. The $P = 0$ limit corresponds to case (V), where $E_{\mathbf{k},\sigma}$ has no zeros and is always positive.

Next, we solve the self-consistency (order parameter and number) equations and analyze the phase diagram at $T = 0$ as a function of scattering parameter $1/(k_{F,+}a_F)$ and population imbalance $P = N_-/N_+$, where $N_\pm = (N_\uparrow \pm N_\downarrow)/2$ and $k_{F,\pm}^3 = (k_{F,\uparrow}^3 \pm k_{F,\downarrow}^3)/2$. We perform calculations for equal ($m_\uparrow = m_\downarrow$) and non-equal ($m_\uparrow = 0.15m_\downarrow$) masses cases, corresponding to one-species (${}^6\text{Li}$ or ${}^{40}\text{K}$ only), and two-species (${}^6\text{Li}$ and ${}^{40}\text{K}$ mixture), respectively.

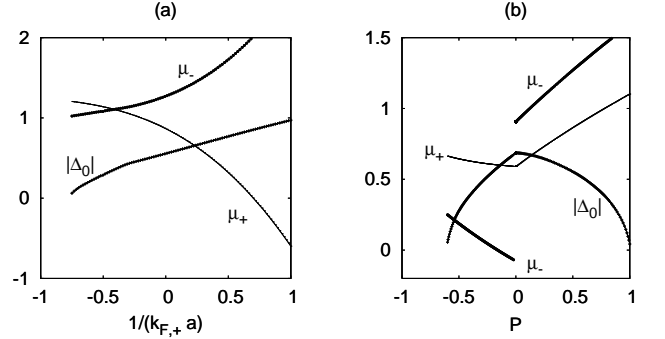


FIG. 2: Plots of $|\Delta_0|$, μ_+ and μ_- (units of $\epsilon_{F,+}$) for $m_\uparrow = 0.15m_\downarrow$ a) as a function of $1/(k_{F,+}a_F)$ when $P = 0.5$ and b) as a function of P when $1/(k_{F,+}a_F) = 0$.

For $T \approx 0$, $N_{\text{fluct},\sigma}$ is small compared to $N_{0,\sigma}$ for all $1/(k_{F,+}a_F)$ leading to $N_\sigma \approx N_{0,\sigma}$ [22]. We define $\epsilon_{F,\pm} = k_{F,\pm}^2/(2m_\pm)$ and in Fig. 2, we plot self-consistent solutions of $|\Delta_0|$, μ_+ and μ_- (in units of $\epsilon_{F,+}$) at $T = 0$ for two cases: a) as a function of $1/(k_{F,+}a_F)$ when $P = 0.5$ (or $N_\uparrow = 3N_\downarrow$) and b) as a function of P when $1/(k_{F,+}a_F) = 0$ (or on resonance). In Fig. 2a, the BCS $\mu_\pm \approx (\epsilon_{F,\uparrow} \pm \epsilon_{F,\downarrow})/2$ changes continuously to the BEC $|\mu_\pm| \rightarrow |\epsilon_b|/2$, where $\epsilon_b = -1/(m_+a_F^2)$ is the binding energy which follows from $1/g = \sum_{\mathbf{k}} |\Gamma_{\mathbf{k}}|^2/(2\epsilon_{\mathbf{k},+} - \epsilon_b)$. Since $P > 0$ and the \uparrow fermions are in excess, all \downarrow fermions pair to form N_\downarrow bosons and the remaining \uparrow fermions are unpaired. The amplitude $|\Delta_0|$ evolves continuously from the BCS to the BEC limit with a cusp around $1/(k_{F,+}a_F) \approx -0.28$. This cusp signals a quantum phase transition from case (II) to case (III) as discussed above, and is more pronounced for higher $|P|$. In Fig. 2b, we show (on resonance) $|\Delta_0| = 0$ (normal phase) for $P < -0.61$, where $\mu_+ \approx 0.64\epsilon_{F,+}$ and $\mu_- \approx 0.28\epsilon_{F,+}$. We notice that the evolution of $|\Delta_0|$, μ_+ and μ_- as a function of P is non-analytic when $|P| \rightarrow 0$, and signals a quantum phase transition from case (III) with $P > 0$

to case (V) with $P = 0$ to case (II) with $P < 0$. We obtain similar results when $m_\uparrow = m_\downarrow$, where the plot is symmetric around $P = 0$. Therefore, this quantum phase transition may be studied in current experiments involving only one-species of fermions [1, 2].

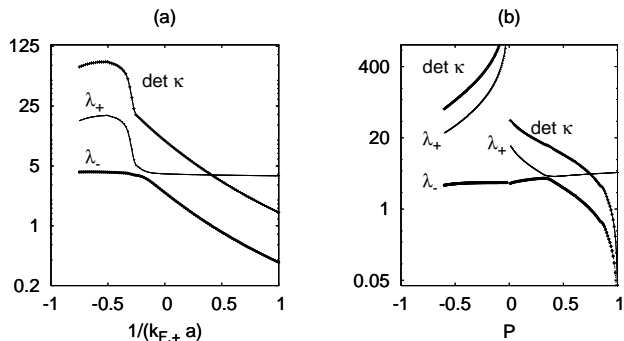


FIG. 3: Plots of $\det \kappa$ (units of $\epsilon_{F,+}^{-2}$), and λ_+ and λ_- (units of $\epsilon_{F,+}^{-1}$) for $m_\uparrow = 0.15m_\downarrow$ a) as a function of $1/(k_{F,+}a_F)$ when $P = 0.5$ and b) as a function of P when $1/(k_{F,+}a_F) = 0$.

Next, we discuss the stability of uniform superfluidity (obtained from the saddle point solutions) using two criteria [9]: positive definite compressibility matrix κ and positive superfluid density $\rho(T)$. The first criterion requires the eigenvalues $\lambda_\pm = \kappa_\pm \pm (\kappa_\pm^2 - \det \kappa)^{1/2}$ of $\kappa_{\sigma,\sigma'} = -\partial^2 \Omega / (\partial \mu_\sigma \partial \mu_{\sigma'})$ to be positive, where $\kappa_\pm = (\kappa_{\uparrow,\uparrow} \pm \kappa_{\downarrow,\downarrow})/2$ and $\det \kappa = \kappa_{\uparrow,\uparrow}\kappa_{\downarrow,\downarrow} - \kappa_{\uparrow,\downarrow}\kappa_{\downarrow,\uparrow}$. At low temperatures ($T \approx 0$) $\kappa_+ = \sum_{\mathbf{k}} [\beta(1 + \xi_{\mathbf{k},+}^2/E_{\mathbf{k},+}^2)\mathcal{Y}_{\mathbf{k},+}/8 + |\Delta_{\mathbf{k}}|^2\mathcal{X}_{\mathbf{k},+}/(2E_{\mathbf{k},+}^3)]$ is positive for all parameter space, and the stability condition reduces only to $\det \kappa > 0$, where $\mathcal{Y}_{\mathbf{k},\sigma} = \text{sech}^2(\beta E_{\mathbf{k},\sigma}/2)$ and $\mathcal{Y}_{\mathbf{k},\pm} = (\mathcal{Y}_{\mathbf{k},\uparrow} \pm \mathcal{Y}_{\mathbf{k},\downarrow})/2$. It can be shown that $\det \kappa = \beta \sum_{\mathbf{k}} \mathcal{Y}_{\mathbf{k},+} \sum_{\mathbf{k}} [|\Delta_{\mathbf{k}}|^2\mathcal{X}_{\mathbf{k},+}/(8E_{\mathbf{k},+}^3) + \beta \xi_{\mathbf{k},+}^2\mathcal{Y}_{\mathbf{k},+}/(16E_{\mathbf{k},+}^2)] - [\beta \sum_{\mathbf{k}} \xi_{\mathbf{k},+}\mathcal{Y}_{\mathbf{k},-}/(4E_{\mathbf{k},+})]^2$, which is also positive for all parameter space at $T \approx 0$. Thus, we conclude that κ is positive definite for all parameter space.

Furthermore, we verify numerically from the matrix elements of κ that $\det \kappa$, λ_+ and λ_- are always positive for all P and $1/(k_{F,+}a_F)$. For instance, in Fig. 3, we plot $\det \kappa$, λ_+ and λ_- for the parameters of Fig. 2. Notice that the eigenvectors corresponding to λ_+ (λ_-) change from out-of-phase (in-phase) to in-phase (out-of-phase) at $1/(k_{F,+}a_F) \approx -0.27$ when $P = 0.5$ leading to an avoided eigenvalue crossing as shown in Fig. 3a. This signals a quantum phase transition from case (II) to case (III) with increasing $1/(k_{F,+}a_F)$ for a fixed P . In addition, at $1/(k_{F,+}a_F) = 0$, all $\det \kappa$, λ_+ and λ_- have non-analyticities in Fig. 3b when $|P| \rightarrow 0$ signalling again a quantum phase transition from case (III) with $P > 0$ to case (V) with $P = 0$ to case (II) with $P < 0$. Notice that, similar phase transitions also exist in the case of equal masses as can be extracted from Fig. 1a.

Next, we discuss the second criterion: positive super-

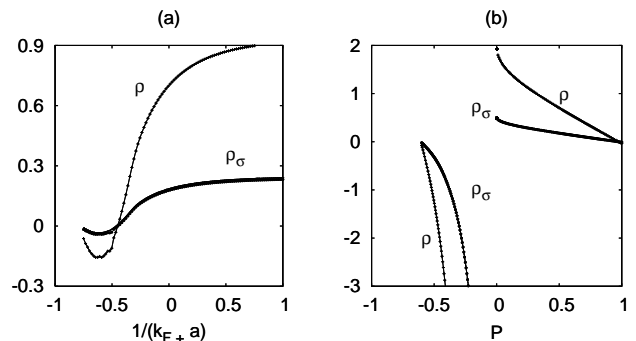


FIG. 4: Plots of $\rho(0)$ (units of m_+N_+) and $\rho_\uparrow(0)$ and $\rho_\downarrow(0)$ (units of N_+) for $m_\uparrow = 0.15m_\downarrow$ a) as a function of $1/(k_{F,+}a_F)$ when $P = 0.5$ and b) as a function of P when $1/(k_{F,+}a_F) = 0$.

fluid density. In general, the superfluid density has a tensor structure $\rho_{ij}(T) = m_\uparrow \rho_{ij,\uparrow}(T) + m_\downarrow \rho_{ij,\downarrow}(T)$ where

$$\rho_{ij,\sigma}(T) = N_\sigma \delta_{ij} - \frac{\beta}{4m_\sigma} \sum_{\mathbf{k}} k_i k_j \left(\mathcal{Y}_{\mathbf{k},+} + s_\sigma \frac{\xi_{\mathbf{k},+}}{E_{\mathbf{k},+}} \mathcal{Y}_{\mathbf{k},-} \right). \quad (5)$$

Here, δ_{ij} is the Kronecker delta. Notice that, in the s-wave case, $\rho_{ij}(T)$ is a scalar given by $\rho(T) = m_\uparrow N_\uparrow + m_\downarrow N_\downarrow - (\beta/6) \sum_{\mathbf{k}} k^2 \mathcal{Y}_{\mathbf{k},+}$. In Fig. 4, we plot $\rho(0)$, $\rho_\uparrow(0)$ and $\rho_\downarrow(0)$ for the parameters of Fig. 2. When $P = 0.5$, the superfluid density is zero for $1/(k_{F,+}a_F) < -0.82$ (normal phase), is negative for $-0.82 < 1/(k_{F,+}a_F) < -0.45$ (unstable phase) and is positive for $1/(k_{F,+}a_F) > -0.45$ (stable phase) as shown in Fig. 4a. When $1/(k_{F,+}a_F) = 0$, the superfluid density is zero for $P < -0.61$ (normal phase), is negative for $-0.61 < P < 0$ and $0.97 < P < 1$ (unstable phase) and is positive for $0 < P < 0.97$ (stable phase) as shown in Fig. 4b.

We perform the same analysis to all P and $1/(k_{F,+}a_F)$ for $m_\uparrow = m_\downarrow$ and $m_\uparrow = 0.15m_\downarrow$, and construct the phase diagrams shown in Fig. 1. In this approximation, a uniform superfluid phase is unstable in the BCS side for arbitrarily small P , and the BCS state is limited only to $P = 0$. Next, we compare our results for equal masses with the recent MIT experiment [1] in a trap. On resonance [$1/(k_{F,+}a_F) = 0$], our unstable uniform superfluid to normal boundary occurs at $P \approx \pm 0.73$ ($\mu_+ \approx 0.93\epsilon_{F,+}$ and $\mu_- \approx \pm 0.51\epsilon_{F,+}$), however the MIT group obtains $P \approx \pm 0.70(4)$ for their superfluid to normal boundary. Furthermore, our stable to unstable uniform superfluid boundary occurs in the BEC side around $|P| \rightarrow 1$, i.e. at $P \approx \pm 0.97$ and ± 0.99 when $1/(k_{F,+}a_F) \approx 0.40$ and 0.75 , respectively, however the MIT group obtains ± 0.95 and ± 0.96 for their superfluid to normal boundary.

Next, we discuss superfluidity near $T \approx T_c$, where $\Delta_0 = 0$, and derive the TDGL equation [23]. We use

the small \mathbf{q} and $iv_\ell \rightarrow \omega + i\delta$ expansion of

$$L^{-1}(q) = \frac{1}{g} - \sum_{\mathbf{k}} \frac{1 - n_F(\xi_{\mathbf{k}+\mathbf{q}/2,\uparrow}) - n_F(\xi_{\mathbf{k}-\mathbf{q}/2,\downarrow})}{\xi_{\mathbf{k}+\mathbf{q}/2,\uparrow} + \xi_{\mathbf{k}-\mathbf{q}/2,\downarrow} - iv_\ell} |\Gamma_{\mathbf{k}}|^2, \quad (6)$$

where $L^{-1}(q) = \mathbf{F}_{11}^{-1}(q)$, to obtain the TDGL equation

$$\left[a + b|\Lambda(x)|^2 - \sum_{i,j} \frac{c_{ij}}{2} \nabla_i \nabla_j - id \frac{\partial}{\partial t} \right] \Lambda(x) = 0 \quad (7)$$

in the real space $x = (\mathbf{x}, t)$ representation. The coefficients are given by $a = 1/g - \sum_{\mathbf{k}} X_{\mathbf{k},+} |\Gamma(\mathbf{k})|^2 / (2\xi_{\mathbf{k},+})$, which leads to the saddle equation when $a = 0$ (Thouless condition), and $c_{ij} = \sum_{\mathbf{k}} \{ \beta^2 k_i k_j (X_{\mathbf{k},\uparrow} Y_{\mathbf{k},\uparrow} / m_\uparrow^2 + X_{\mathbf{k},\downarrow} Y_{\mathbf{k},\downarrow} / m_\downarrow^2) / (32\xi_{\mathbf{k},+}) + \beta(k_i k_j C_- / m_- - \delta_{ij} C_+ / 2) (8\xi_{\mathbf{k},+}^2) + X_{\mathbf{k},+} [\delta_{ij} / (2m_+) - k_i k_j / (m_-^2 \xi_{\mathbf{k},+})] / (4\xi_{\mathbf{k},+}^2) \} |\Gamma_{\mathbf{k}}|^2$, where $C_\pm = (Y_{\mathbf{k},\uparrow} / m_\uparrow \pm Y_{\mathbf{k},\downarrow} / m_\downarrow) / 2$, $X_{\mathbf{k},\sigma} = \tanh(\beta\xi_{\mathbf{k},\sigma} / 2)$ and $Y_{\mathbf{k},\sigma} = \text{sech}^2(\beta\xi_{\mathbf{k},\sigma} / 2)$. Notice that c_{ij} reduces to a scalar c in the s-wave case. The coefficient of the nonlinear term is $b = \sum_{\mathbf{k}} [X_{\mathbf{k},+} / (4\xi_{\mathbf{k},+}^3) - \beta Y_{\mathbf{k},+} / (8\xi_{\mathbf{k},+}^2)] |\Gamma_{\mathbf{k}}|^4$, while d has real and imaginary parts given by $d = \lim_{w \rightarrow 0} \sum_{\mathbf{k}} X_{\mathbf{k},+} [1 / (8\xi_{\mathbf{k},+}^2) + i\pi\delta(2\xi_{\mathbf{k},+} - w) / (2w)] |\Gamma_{\mathbf{k}}|^2$, where $\delta(x)$ is the Delta function. Notice that the damping term (imaginary part of d) vanishes for $\mu_+ \leq 0$, indicating an undamped dynamics for $\Lambda(x)$.

Since a uniform superfluid phase is more stable in the BEC side, we calculate analytically all coefficients in the BEC limit where $|\mu_\pm| \sim |\epsilon_b|/2 \gg T_c$. We obtain $a = a_1 + a_2 = -Vm_+^2(2\mu_+ - \epsilon_b)a_F / (8\pi) + Vm_+n_e a_F^2$, $b = b_1 + b_2 = Vm_+^3 a_F^3 / (16\pi) - Vm_+^2 (\partial n_e / \partial \mu_e) a_F^4$, $c = Vm_+^2 a_F / [8\pi(m_\uparrow + m_\downarrow)]$, and $d = Vm_+^2 a_F / (8\pi)$. Here, e labels the excess type of fermions and n_e is the density of unpaired fermions. Through the rescaling $\Psi(x) = \sqrt{d}\Lambda(x)$, we obtain the equation of motion for a dilute mixture of weakly interacting bosons and fermions

$$\mu_B \Psi(x) + [U_{BB}|\Psi(x)|^2 + U_{BF}n_e(x)] \Psi(x) - \frac{\nabla^2 \Psi(x)}{2m_B} - i \frac{\partial \Psi(x)}{\partial t} = 0, \quad (8)$$

with bosonic chemical potential $\mu_B = -a_1/d = 2\mu_+ - \epsilon_b$, mass $m_B = d/c = m_\uparrow + m_\downarrow$, and repulsive boson-boson $U_{BB} = b_1/d^2 = 4\pi a_F / (m_+ V)$ and boson-fermion $U_{BF} = a_1 / (dn_e) = 8\pi a_F / (m_+ V)$ interactions. This procedure also yields the spatial density of unpaired fermions given by $n_e(x) = [a_2/d + b_2|\Psi(x)|^2/d^2] / U_{BF} = n_e - 8\pi a_F (\partial n_e / \partial \mu_e) |\Psi(x)|^2 / (Vm_+)$. Since $\partial n_e / \partial \mu_e > 0$ the unpaired fermions avoid regions where the boson field $|\psi(x)|$ is large. Thus, the bosons condense at the center and the unpaired fermions tend to be at the edges in a trap. Notice that, Eq. (8) reduces to the Gross-Pitaevskii equation for equal masses with $P = 0$ [23], and to the equation of motion for equal masses with $P \neq 0$ [15].

Furthermore, we obtain the boson-boson $a_{BB} = [1 + m_\uparrow / (2m_\downarrow) + m_\downarrow / (2m_\uparrow)] a_F$ and boson-fermion $a_{BF} =$

$4m_B m_e / [m_+ (m_B + m_e)] a_F$ scattering lengths, which reduce to $a_{BB} = 2a_F$ and $a_{BF} = 8a_F/3$ for equal masses [15, 23]. For a mixture of ${}^6\text{Li}$ and ${}^{40}\text{K}$, $a_{BB} \approx 4.41a_F$, and $a_{BF} \approx 2.03a_F$ when ${}^6\text{Li}$ is in excess, and $a_{BF} \approx 8.20a_F$ when ${}^{40}\text{K}$ is in excess. Our results are obtained in the Born approximation, but higher order scattering processes are needed for a better estimate [24]. Since the effective boson-fermion system is weakly interacting, the BEC temperature is $T_c = \pi[n_B/\zeta(3/2)]^{2/3}/m_B$, where $\zeta(x)$ is the Zeta function and $n_B = (n - n_e)/2$.

In summary, we analyzed the phase diagram of uniform superfluidity for two-species fermion mixtures (e.g. ${}^6\text{Li}$ and ${}^{40}\text{K}$) from the BCS to the BEC limit as a function of scattering parameter and population imbalance. We found that the zero temperature phase diagram of population imbalance versus scattering parameter is asymmetric for non-equal masses, having a larger stability region for uniform superfluidity when the lighter fermions are in excess. This result is in sharp contrast with the symmetric phase diagram for equal masses. In addition, we found topological quantum phase transitions associated with the disappearance or appearance of momentum space regions of zero quasiparticle energies. Near the critical temperature, we derived the Ginzburg-Landau equation, and showed that it describes a dilute mixture of bosons (tightly bound fermions) and excess (unpaired) fermions in the BEC limit.

We thank NSF (DMR-0304380) for support.

-
- [1] M. W. Zwierlein et al., Science **311**, 492 (2006).
 - [2] G. B. Partridge et al., Science **311**, 503 (2006).
 - [3] C. A. Regal et al., Phys. Rev. Lett. **92**, 040403 (2004).
 - [4] M. Bartenstein et al., Phys. Rev. Lett. **92**, 120401 (2004).
 - [5] J. Kinast et al., Phys. Rev. Lett. **92**, 150402 (2004).
 - [6] T. Bourdel et al., Phys. Rev. Lett. **93**, 050401 (2004).
 - [7] M. Köhl et al., Phys. Rev. Lett. **94**, 080403 (2005).
 - [8] J. Carlson and S. Reddy, Phys. Rev. Lett. **95**, 060401 (2005).
 - [9] C. H. Pao et al., cond-mat/0506437.
 - [10] D. T. Son and M. A. Stephanov, cond-mat/0507586.
 - [11] D. E. Sheehy and L. Radzihovsky, Phys. Rev. Lett. **96**, 060401 (2006).
 - [12] T. L. Ho and H. Zhai, cond-mat/0602568.
 - [13] Z.-C. Gu et al., cond-mat/0603091.
 - [14] Hui Hu and Xia-Ji Lu, cond-mat/0603332.
 - [15] P. Pieri and G. C. Strinati, cond-mat/0512354.
 - [16] W. Yi and L. M. Duan, cond-mat/0601006.
 - [17] F. Chevy, cond-mat/0601122.
 - [18] T. N. De Silva and E. J. Mueller, cond-mat/0601314.
 - [19] M. Haque and H. T. C. Stoof, cond-mat/0601321.
 - [20] W. V. Liu and F. Wilczek, Phys. Rev. Lett. **90**, 047002 (2003).
 - [21] P. F. Bedaque et al., Phys. Rev. Lett. **91**, 247002 (2003).
 - [22] J. R. Engelbrecht et al., Phys. Rev. B **55**, 15153 (1997).
 - [23] C. A. R. Sá de Melo et al., Phys. Rev. Lett. **71**, 3202

(1993).
[24] D. S. Petrov et al., J. Phys. B: At. Mol. Opt. Phys. **38**,

S645 (2005).